

Bromine Is an Essential Trace Element for Assembly of Collagen IV Scaffolds in Tissue Development and Architecture

A. Scott McCall,^{1,10} Christopher F. Cummings,^{2,3,10} Gautam Bhavé,^{3,10} Roberto Vanacore,^{3,4} Andrea Page-McCaw,^{5,6,7} and Billy G. Hudson^{2,3,4,7,8,9,*}

¹Department of Pharmacology, Vanderbilt University School of Medicine, 451 Preston Research Building, Nashville, TN 37232, USA

²Department of Biochemistry, Vanderbilt University School of Medicine, 607 Light Hall, Nashville, TN 37232, USA

³Division of Nephrology and Hypertension, Department of Medicine, Vanderbilt University School of Medicine, D-3100 Medical Center North, Nashville, TN 37232, USA

⁴Center for Matrix Biology, Vanderbilt University Medical Center, 1161 21st Avenue South, Nashville, TN 37232, USA

⁵Department of Cell and Developmental Biology, Vanderbilt University School of Medicine, U-3218 Medical Research Building III, Nashville, TN 37232, USA

⁶Department of Cancer Biology, Vanderbilt University School of Medicine, 691 Preston Research Building, Nashville, TN 37232, USA

⁷Vanderbilt Ingram Cancer Center, Vanderbilt University Medical Center, 2220 Pierce Avenue, Nashville, TN 37232, USA

⁸Department of Pathology, Microbiology, and Immunology, Vanderbilt University School of Medicine, C-3322 Medical Center North, Nashville, TN 37232, USA

⁹Vanderbilt Institute of Chemical Biology, Vanderbilt University Medical Center, 896 Preston Research Building, Nashville, TN 37232, USA

¹⁰Co-first author

*Correspondence: billy.hudson@vanderbilt.edu

<http://dx.doi.org/10.1016/j.cell.2014.05.009>

SUMMARY

Bromine is ubiquitously present in animals as ionic bromide (Br^-) yet has no known essential function. Herein, we demonstrate that Br^- is a required cofactor for peroxidase-catalyzed formation of sulfilimine crosslinks, a posttranslational modification essential for tissue development and architecture found within the collagen IV scaffold of basement membranes (BMs). Bromide, converted to hypobromous acid, forms a bromosulfonium-ion intermediate that energetically selects for sulfilimine formation. Dietary Br deficiency is lethal in *Drosophila*, whereas Br replenishment restores viability, demonstrating its physiologic requirement. Importantly, Br-deficient flies phenocopy the developmental and BM defects observed in peroxidase mutants and indicate a functional connection between Br^- , collagen IV, and peroxidase. We establish that Br^- is required for sulfilimine formation within collagen IV, an event critical for BM assembly and tissue development. Thus, bromine is an essential trace element for all animals, and its deficiency may be relevant to BM alterations observed in nutritional and smoking-related disease.

INTRODUCTION

Basement membranes (BMs) are specialized extracellular matrices that are key mediators of signal transduction and mechanical support for epithelial cells (Daley and Yamada, 2013;

Hynes, 2009; Lin and Bissell, 1993; Werb, 1997; Yurchenco, 2011). Indeed, BMs coordinate branching morphogenesis and define epithelial tissue architecture, facilitate tissue repair after injury, and guide pluripotent cells in tissue-engineered organ regeneration (Song and Ott, 2011; Vracko, 1974). Embedded within the BM is a sulfilimine-crosslinked collagen IV scaffold that imparts functionality to the matrix of multicellular tissues in all animal phyla (Bhavé et al., 2012; Fidler et al., 2014; Vanacore et al., 2009). Collagen IV scaffolds provide mechanical strength, serve as a ligand for integrins and other cell-surface receptors, and interact with growth factors such as BMPs to establish signaling gradients (Wang et al., 2008). Mutations in the collagen IV scaffold cause BM destabilization and tissue dysfunction in humans, nematodes, flies, and mice (Borchiellini et al., 1996; Gould et al., 2005; Gupta et al., 1997; Hudson et al., 2003; Pastor-Pareja and Xu, 2011; Pöschl et al., 2004; Rodriguez et al., 1996).

Assembly of the collagen IV scaffold is an intricate process of organization and covalent reinforcement. Triple-helical protomers extracellularly self-assemble into insoluble lattices, and nascent scaffolds are stabilized via the enzymatic formation of sulfilimine crosslinks between the NC1 domains of two juxtaposed protomers at residues methionine 93 (Met^{93}) and hydroxylysine 211 (Hyl^{211}) (Vanacore et al., 2009) (Figure 1A). Peroxidase, a heme peroxidase embedded within BMs, catalyzes the formation of sulfilimine crosslinks, which confer critical structural reinforcement to collagen IV scaffolds, as seen in nematodes, flies, and zebrafish, where loss of peroxidase causes BM dysfunction (Bhavé et al., 2012; Fidler et al., 2014; Gotenstein et al., 2010).

Peroxidase forms hypobromous acid (HOBr) and hypochlorous acid (HOCl) from bromide and chloride, respectively, both

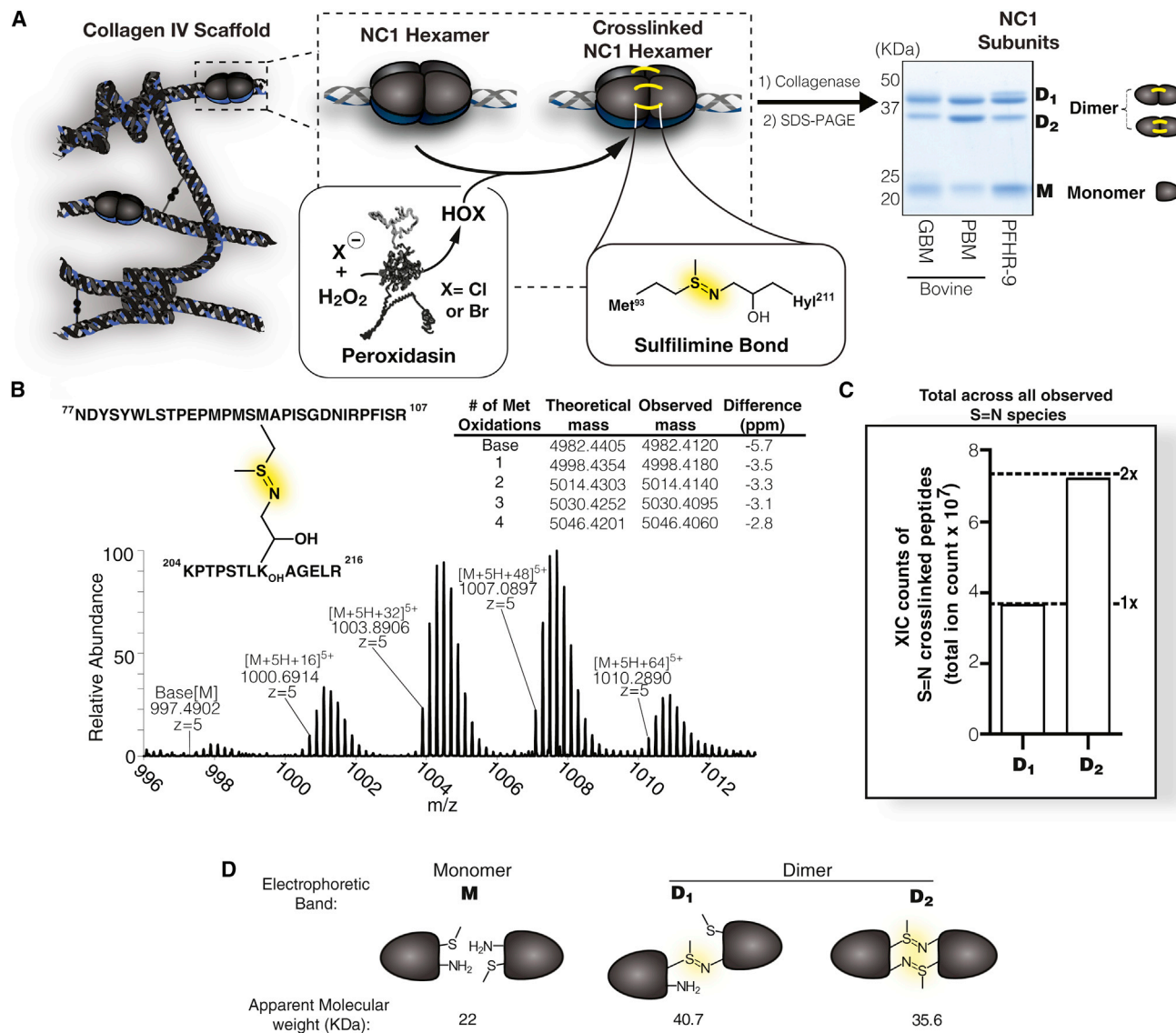


Figure 1. Measurement of Sulfilimine-Crosslink Content within NC1 Domains of Collagen IV Scaffolds

(A) Diagram of the collagen IV scaffold, showing the relationship of NC1 hexamer sulfilimine crosslinks, peroxidase (PXDN), and hypohalous acids (HOX). Inset shows resolution of dimeric (D₁ and D₂) and monomeric (M) NC1 domains by SDS-PAGE. Representative NC1 domains are shown from bovine placental BM (PBM), bovine glomerular BM (GBM), and murine collagen IV matrix produced in PFHR-9 cell culture.

(B) High-resolution mass spectrum depicting the multiple oxidation states of tryptic peptides containing the sulfilimine (S = N) crosslink.

(C) Extracted ion current (XIC) based quantitation of S = N crosslinked peptides from D₁ and D₂. Full data appear in [Figure S1](#).

(D) Diagram showing the crosslinking status of observed NC1 banding in SDS-PAGE, where D₁ is singly crosslinked and D₂ is doubly crosslinked with a resultant higher electrophoretic mobility.

of which can mediate crosslink formation ([Figure 1A](#)). In vitro studies point to a preference for Br⁻ during enzymatic sulfilimine formation, but its role within the in vivo reaction is unknown, particularly in light of the vast excess of Cl⁻ over Br⁻ in most animals ([Weiss et al., 1986](#)). Despite its ubiquitous yet trace presence within animals, Br⁻ is without a known essential function. Bromide is a cofactor for eosinophil peroxidase (EPO) following eosinophil activation ([Mayeno et al., 1989](#); [Weiss et al., 1986](#)), but the relevance of this is unclear as EPO preferentially oxidizes SCN⁻ over Br⁻ ([Nagy et al., 2006](#)). Thus, the definitive identifica-

tion of Br⁻ as a cofactor for peroxidase-mediated crosslink formation would represent the first essential function for the element bromine.

Herein, we generated Br-free Cl⁻ salts and found that peroxidase uses Br⁻ to catalyze formation of sulfilimine crosslinks with at least 50,000-fold greater efficiency compared to Cl⁻. *Drosophila* raised on Br-deficient diets resemble peroxidase loss-of-function mutations, including developmental abnormalities, lethality, and altered BM and tissue morphologies. Importantly, replenishment of Br⁻ to the diet restores the normal

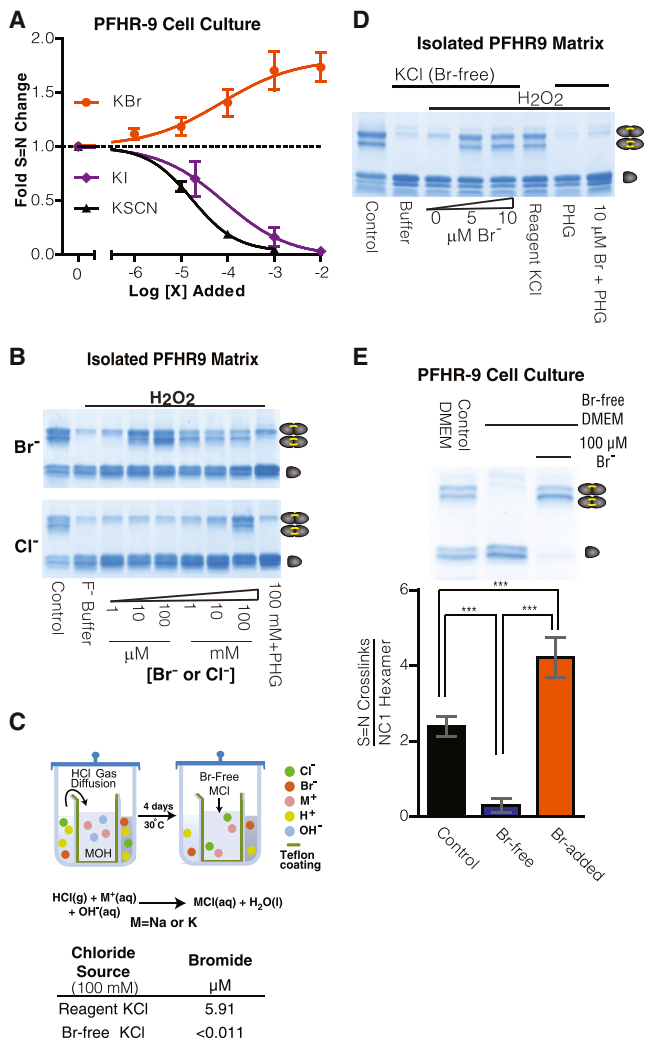


Figure 2. Bromide Is the Required Cofactor for Sulfilimine-Crosslink Formation

(A) The effect of halide ions on sulfilimine-crosslink formation is examined in PFHR-9 matrix. Inhibition values were calculated from nonlinear curve fitting: KI ($\text{IC}_{50} = 84 \mu\text{M}$ 95%CI [30–241 μM]), KSCN ($\text{IC}_{50} = 17 \mu\text{M}$ 95%CI [3–24 μM]). Contrasting with these effects, exogenous potassium bromide (KBr) enhanced the reaction. Points represent mean \pm SD ($n = 3$). See also Figure S2.

(B) Uncrosslinked PFHR9 matrix was crosslinked *in vitro* in the presence of KCl and KBr and reacted for 1 hr at 37°C with 1 mM H_2O_2 , with 100 mM KF used as ionic strength control. Collagenase digest was analyzed by SDS-PAGE and Coomassie staining.

(C) Schematic of Br-free Cl^- salt purification apparatus and setup. Resulting salt was analyzed by ICP-MS for bromide content. Further analysis of salt reagents appears in Table S1 and Figure S3.

(D) Crosslink formation in PFHR-9 matrix with Br-free KCl. Reaction buffer contained 10 mM phosphate buffer (pH 7.4), 100 mM Br-free or reagent-grade KCl, and 1 mM H_2O_2 and 200 μM PHG where appropriate. Displayed SDS-PAGE gels were stained with Coomassie blue.

(E) Sulfilimine (S=N) crosslink formation in PFHR-9 cell culture tested under Br-free conditions. Culture conditions and media formulations are presented in detail in the Extended Experimental Procedures. NC1 hexamers were isolated via collagenase treatment and analyzed by SDS-PAGE. The amount of crosslinks per hexamer is graphed as the mean \pm 95% CI ($n = 3$). All sample groups had equal variance, one-way ANOVA was performed ($p < 0.001$), and differences between groups were tested with Tukey's post-hoc analysis (** $p < 0.001$).

phenotype in all metrics addressed here. Collectively, our findings establish a physiologic requirement for Br^- in animals, the mechanism by which Br^- functions, and the essentiality of a sulfilimine-crosslinked collagen IV scaffold in the assembly and function of BMs.

RESULTS

Structural Basis for Sulfilimine-Crosslink Heterogeneity in the Collagen IV Scaffold

Sulfilimine crosslinks join NC1 domains at the interface of two adjoining triple helical protomers within the collagen IV scaffold, forming a globular hexameric structure. Dimerized NC1 domains may be bound together by either one or two sulfilimine crosslinks, due to the presence of Met⁹³ and Hyl²¹¹ in both domains. Following biochemical isolation and SDS-PAGE analysis, NC1 hexamers dissociate into crosslinked dimers, termed D₁ and D₂, and uncrosslinked monomers (Figure 1A). The structural distinction between D₁ and D₂ is unknown but of long-standing interest (Langeveld et al., 1988). Because HOBr reacts with uncrosslinked NC1 hexamer to uniquely form D₂ with a pattern resembling native placental and glomerular BMs, we endeavored to structurally define the D₁ and D₂ isoforms of crosslinked hexamer. We hypothesized that D₁ and D₂ differed by the number of crosslinks, D₁ having one and D₂ with two crosslinks. Using liquid chromatography-mass spectrometry (LC-MS) to determine the abundance of crosslinks in D₁ and D₂, we found 1.95 times greater sulfilimine-containing peptides in D₂ relative to D₁ (Figures 1B and 1C and Figure S1 available online), indicating that D₂ has two crosslinks and D₁ has one. We thus used the relative abundance of D₁ and D₂ on SDS-PAGE analysis of NC1 hexamers to assess sulfilimine-crosslink content (Figure 1D).

Bromide Is Required for Sulfilimine Formation

We next examined the effect of halides (F^- , Cl^- , Br^- , I^-) and the pseudohalide thiocyanate (SCN^-) on sulfilimine crosslinking in cell culture. SCN^- and I^- inhibited the reaction, whereas Br^- enhanced crosslink formation (Figures 2A and S2). Because F^- proved cytotoxic, and background levels in media precluded testing of Cl^- , we moved to isolated PFHR-9 BM as an *in vitro* model for crosslink formation. In this model, KI inhibits peroxidase to generate an uncrosslinked scaffold, and subsequent KI removal with addition of H_2O_2 drives crosslink formation by peroxidase. (Bhave et al., 2012). F^- was inert to crosslink formation, so we used 100 mM KF as an ionic control while titrating either Cl^- or Br^- (Figure 2B). Br^- robustly catalyzed crosslink formation at 10 μM , whereas Cl^- remained inactive until 100 mM (Figure 2B).

Although these data pointed to a strong preference for Br^- over Cl^- in crosslink formation, we considered whether contaminating Br^- in our Cl^- solutions might confound the results. Indeed, we measured Br^- content at 5.91 μM /100 mM KCl (inductively coupled plasma-mass spectrometry [ICP-MS]) (Table S1), making the apparent Cl^- activity difficult to distinguish from that of contaminating Br^- . To address this, we produced Br-free NaCl and KCl (<11.4 nM Br^-) (Figures 2C and S3A; Table S1). Intriguingly, Br-free Cl^- did not support crosslink formation (Figures 2D and S3B), whereas addition of 5 μM Br^- rescued crosslink formation.

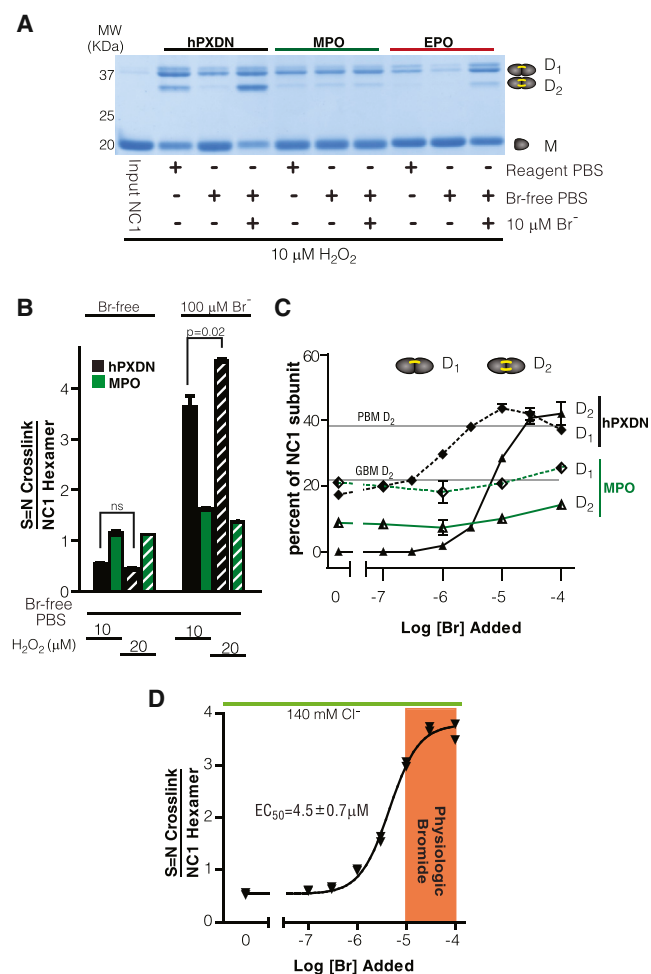


Figure 3. Peroxidase Uses Physiologic Br^- Levels to Form Sulfilimine Crosslinks

(A–D) Mammalian peroxidases are compared for ability to crosslink collagen IV NC1 domains in Br-free $1 \times$ PBS, recombinant human peroxidase (hPXDN), myeloperoxidase (MPO), and eosinophilperoxidase (EPO). Uncrosslinked NC1 domains were isolated from PHG-treated PFHR-9 cultures. All peroxidase activity enzymes were normalized by TMB assay prior to assay (Bozeman et al., 1990). Reactions proceeded for 10 min at 37°C after initiation by the addition of H_2O_2 and quenched with 5 mM PHG, 0.2 mg/ml bovine catalase, and 10 mM methionine. Gel is representative of three experiments.

(A) Coomassie-stained gel of enzymatic crosslink formation under reagent-grade and Br-free conditions.

(B) Quantitative analysis of crosslinks formed per NC1 hexamer by MPO and hPXDN under Br-free and Br-added (100 μM) conditions. Data shown as mean \pm 1 SD, $n = 2$. Student's t test was performed ($n = 2$) due to equal variance between groups.

(C) Effect of bromide titration on the proportion of D₁ (one crosslink) and D₂ (two crosslinks) NC1 populations following reaction with MPO and hPXDN. For reference, the proportions of D₂ found in PBM and GBM are denoted on the graph. Data shown as mean \pm 1 SD ($n = 2$).

(D) Crosslinking efficacy of peroxidase measured as crosslink formed per hexamer upon Br^- titration. EC_{50} value \pm 95% CI ($n = 2$).

For validation, we tested the efficiency of crosslink formation in PFHR-9 cells grown in Br-free media ($<2.5 \mu\text{M Br}^-$, as measured by neutron activation analysis [NAA]; Tables S2–S4).

In Br-free and Br-added culture conditions, there was no appreciable difference in cell proliferation, cell viability, or collagen IV production. Importantly, Br⁻-free media did not support formation of crosslinks in the collagen IV matrix, yet the addition of 100 $\mu\text{M Br}^-$ to the same media rescued normal crosslink formation (Figure 2E), establishing a requirement for Br⁻ in sulfilimine formation.

Peroxidase Catalyzes Sulfilimine-Crosslink Formation via Bromide

Continuing our studies with purified Cl⁻, we examined the sulfilimine formation capability of peroxidase, myeloperoxidase (MPO), and EPO in Br-free conditions. Generally, peroxidases use peroxide to oxidize a halide ion to the corresponding hypohalous acid (HOX, X = Cl or Br) with MPO preferentially oxidizing Cl⁻ to HOCl and peroxidase and EPO forming HOBr via oxidation of Br⁻. After normalization of peroxidase activity of all enzyme preparations (Bozeman et al., 1990), we found peroxidase to be much more effective in forming sulfilimine crosslinks within NC1 hexamers than MPO or EPO under identical conditions, especially regarding D₂ (two crosslinks) formation (Figure 3A). Crosslinking by peroxidase exceeded EPO despite normalized enzyme activity.

We sought to characterize the responsiveness of peroxidase and MPO to Br⁻ levels. In Br-free saline, where HOCl is the only hypohalous product of either enzyme, only minor amounts of crosslink were produced by the enzymes. The addition of 100 $\mu\text{M Br}^-$ significantly enhanced crosslink formation by peroxidase, as did increased H_2O_2 levels (Figure 3B), suggesting that the in vivo enzymatic mechanism is responsive to both Br⁻ and oxidant concentrations. Upon Br⁻ titration, D₁ formed prior to D₂, indicating a sequential crosslinking mechanism (Figure 3C), complementing our LC-MS studies that revealed one and two sulfilimine crosslinks in D₁ and D₂, respectively (Figures 1B and 1C). Thus, the relative amount of D₂ represents a key index of crosslinks within the overall NC1 hexamer and is a notable feature of tissue-isolated collagen IV (Figure S4) (Langeveld et al., 1988). In vitro, we found that crosslink formation by either a Br- H_2O_2 -peroxidase system or the direct HOBr application produces D₂ to a similar degree as observed in tissues (Figure S4).

Considering the trace levels of Br⁻ in physiology, we calculated the EC_{50} for Br⁻ in this system to be 4.5 μM (95% confidence interval [CI] 3.8–5.2 μM) in the presence of 140 mM Cl⁻ (Figure 3D). Using MPO as a baseline for the efficacy of Cl⁻-based oxidants, these data indicate a $> 50,000$ -fold efficacy difference for Br⁻ over Cl⁻ as a cofactor in the peroxidase-catalyzed formation of crosslinks, demonstrating selectivity for Br⁻. Within the normal serum range of 10–100 $\mu\text{M Br}^-$ (van Leeuwen and Sangster, 1987), peroxidase formed crosslinks at more than 90% of the available sites but was markedly less effective below this range, indicating an optimal Br⁻ level for in vivo crosslink formation.

The Chemical Basis for Selection of Br⁻ over Cl⁻ as the Cofactor in Crosslink Formation

To investigate the chemical basis for the selectivity of Br⁻ over Cl⁻ in this reaction, we used the halogen-based synthesis of

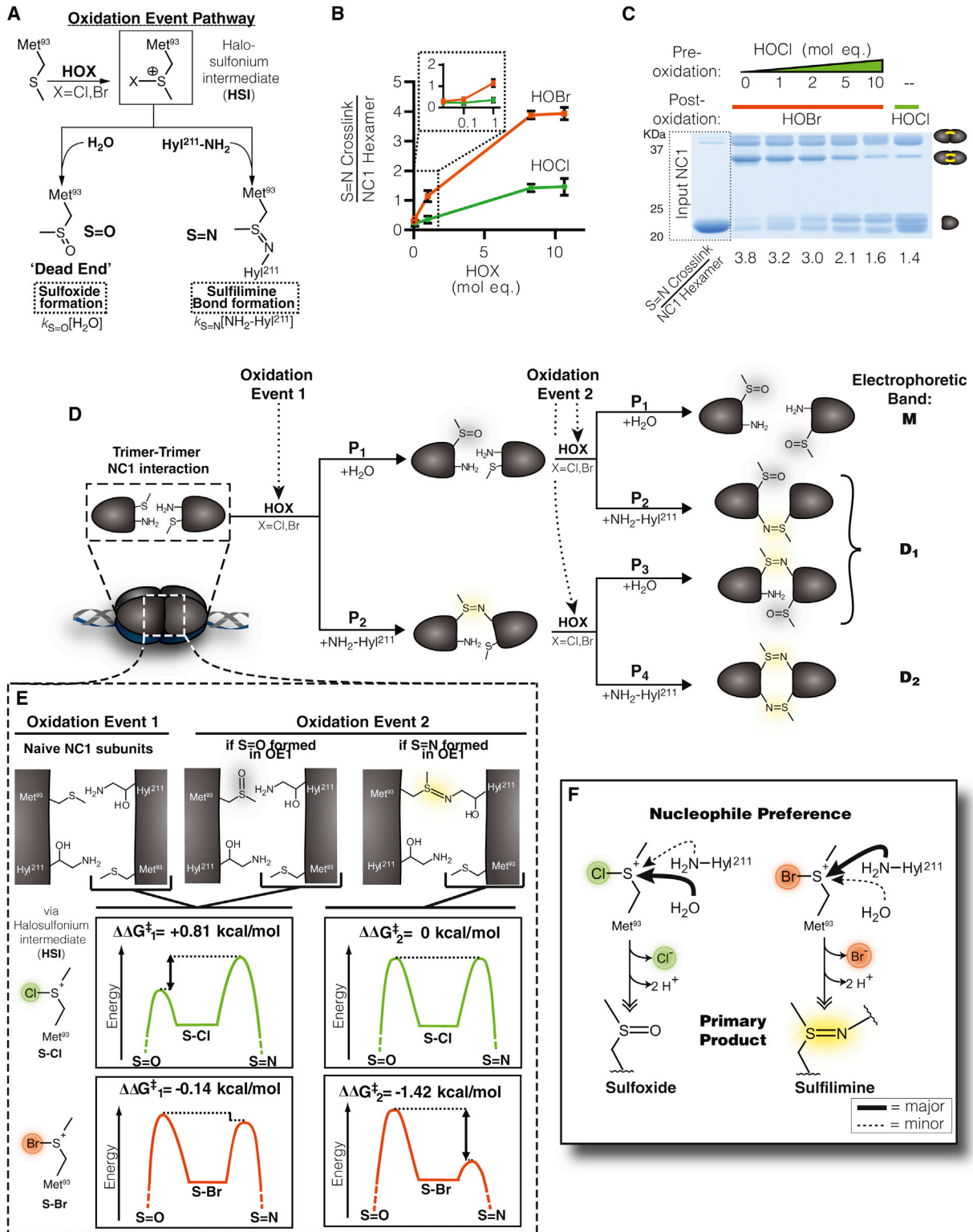


Figure 4. Chemical Mechanism of Sulfilimine Formation within the NC1 Hexamer

(A) Working model of the oxidative formation of either sulfilimine crosslinks or methionine sulfoxide. $k_{S=O}$ and $k_{S=N}$ refer to rate constants in the formation of sulfoxides and sulfilimines, respectively.

(B) Uncrosslinked NC1 hexamers (5 μ M) were reacted with hypohalous acids for 5 min at 37°C, and the products analyzed by SDS-PAGE. Values represent mean \pm 95% CI (n = 3).

(legend continued on next page)

dehydromethionine, a cyclic sulfilimine product, as a mechanistic framework wherein a methionine halosulfonium intermediate (HSI) reacts with either an amine or water to form a sulfilimine bond or sulfoxide, respectively (Figure 4A) (Armesto et al., 2000; Peskin et al., 2009; Young and Hsieh, 1978). We hypothesized that (1) collagen IV sulfilimine bond formation proceeds via an HSI at Met⁹³, and (2) selectivity resides with a bromosulfonium intermediate that predominately reacts with the ϵ -NH₂ of Hyl²¹¹ to form the crosslink, whereas the chlorosulfonium intermediate predominantly reacts with water to form methionine sulfoxide, precluding crosslink formation.

In vitro, HOBr effectively promoted crosslink formation in a dose-dependent manner, whereas HOCl poorly formed NC1 crosslinks (Figure 4B). We used mass spectrometry to determine the oxidation state of Met⁹³ within HOCl-reacted monomers and found increased amounts of methionine sulfoxide (Figure S5). To test whether methionine sulfoxide is indeed a “dead end” with respect to crosslink formation, we treated uncrosslinked NC1 hexamers with HOCl prior to HOBr treatment and found a dose-dependent inhibition of crosslink formation until it resembled treatment with HOCl alone (Figure 4C). Thus, both HOBr and HOCl target Met⁹³, yet the latter oxidant creates an uncrosslinkable product, namely methionine sulfoxide. As further validation, similar results were obtained when sulfoxide was generated using prolonged treatment with high concentrations of H₂O₂ (Figure S5G).

Probing deeper into the mechanism, we sought to characterize the reactivity and energetics of Met⁹³ after oxidation with HOBr or HOCl. We modeled distinct HSI reaction pathways yielding sulfoxide or sulfilimine and two potential crosslinking events between opposing NC1 subunits (Figures 4D and S6). Using densitometric analysis of SDS-PAGE gels, we measured the relative proportion of uncrosslinked, singly crosslinked, and doubly crosslinked NC1 subunits following complete oxidation with either HOBr or HOCl to calculate the sulfilimine and sulfoxide product ratios for both oxidative events (Figures S6C and S6D). The data indicated that the two oxidation events are not independent (Table S5), but rather, formation of the first sulfilimine enhances the probability of a second crosslinking event. Possible physical interpretations of these data are that the first crosslink imposes steric constraints on the orientation of Met⁹³ and Hyl²¹¹ at the second site or simply increases their spatial proximity such that the apparent local amine concentration increases 3- to 7-fold (see Extended Experimental Procedures). We examined the relative free-energy difference in the transition states for the competing sulfilimine and sulfoxide reaction pathways (Figures 4E and S6B–S6D; Extended Experimental Procedures) (Seeman, 1983) and found that the bromosulfonium (**S-Br**) intermediate encountered a lower energetic barrier to sulfilimine formation for both oxidative events, whereas

the chlorosulfonium (**S-Cl**) intermediate faced an unfavorable barrier to sulfilimine formation relative to methionine sulfoxide (Figures 4E and S6D).

Further explanation for the difference in products between Br⁻ and Cl⁻ in collagen IV may be found in the distinct chemical behaviors of **S-Br** and **S-Cl**. Experimental and in silico studies indicate that **S-Cl** species have highly polar transition states and therefore participate in charge-controlled reactions that prefer “harder” nucleophiles such as H₂O relative to amine and thereby favor sulfoxide formation. Conversely, **S-Br** species generate transition states with smaller partial charge, which favor orbital-controlled reactions that select for “softer” nucleophiles (here understood as NH₂-R relative to H₂O) and thus prefer sulfilimine formation (Chmutova et al., 1999; Klopman, 1968; Pearson, 1968). Taken together, sulfilimine formation is thermodynamically favorable via the selectivity of an **S-Br** intermediate at Met⁹³, providing chemical basis for the Br⁻ requirement.

Bromide Is Essential for *Drosophila* Development

Based on the chemical requirement for Br⁻ in collagen IV sulfilimine bond formation and the conservation of the crosslink in multicellular tissues (Fidler et al., 2014), we hypothesized that Br⁻ is essential for stabilizing tissues. We tested this hypothesis in *Drosophila*. Because standard *Drosophila* media contains ~15 μ M Br⁻, we prepared a custom diet (Table S7) in which final dietary Br⁻ was undetectable by NAA (Table S2). To address the impact of Br⁻ deficiency over multiple generations, we raised flies on Br-free media and compared their development to cohorts raised on either similar media with Br⁻ supplementation or standard media (Figure 5A). Initial maternal Br⁻ contribution in embryos was 24.3 μ M (Table S2) on the standard diet. After moving embryos to the indicated media, Generation 1 larvae grown on Br-free conditions exhibited developmental delay (Figure 5B), yet development rates were similar between Br-added and standard media. Adult Generation 1 flies that survived were maintained on the same diet for 14 days to continue Br⁻ depletion, and progeny Generation 2 larvae showed significantly reduced survival in Br-free versus standard; the phenotype was rescued in Br-added diet (Figure 5C). Thus, Br⁻ is essential for development in *Drosophila*.

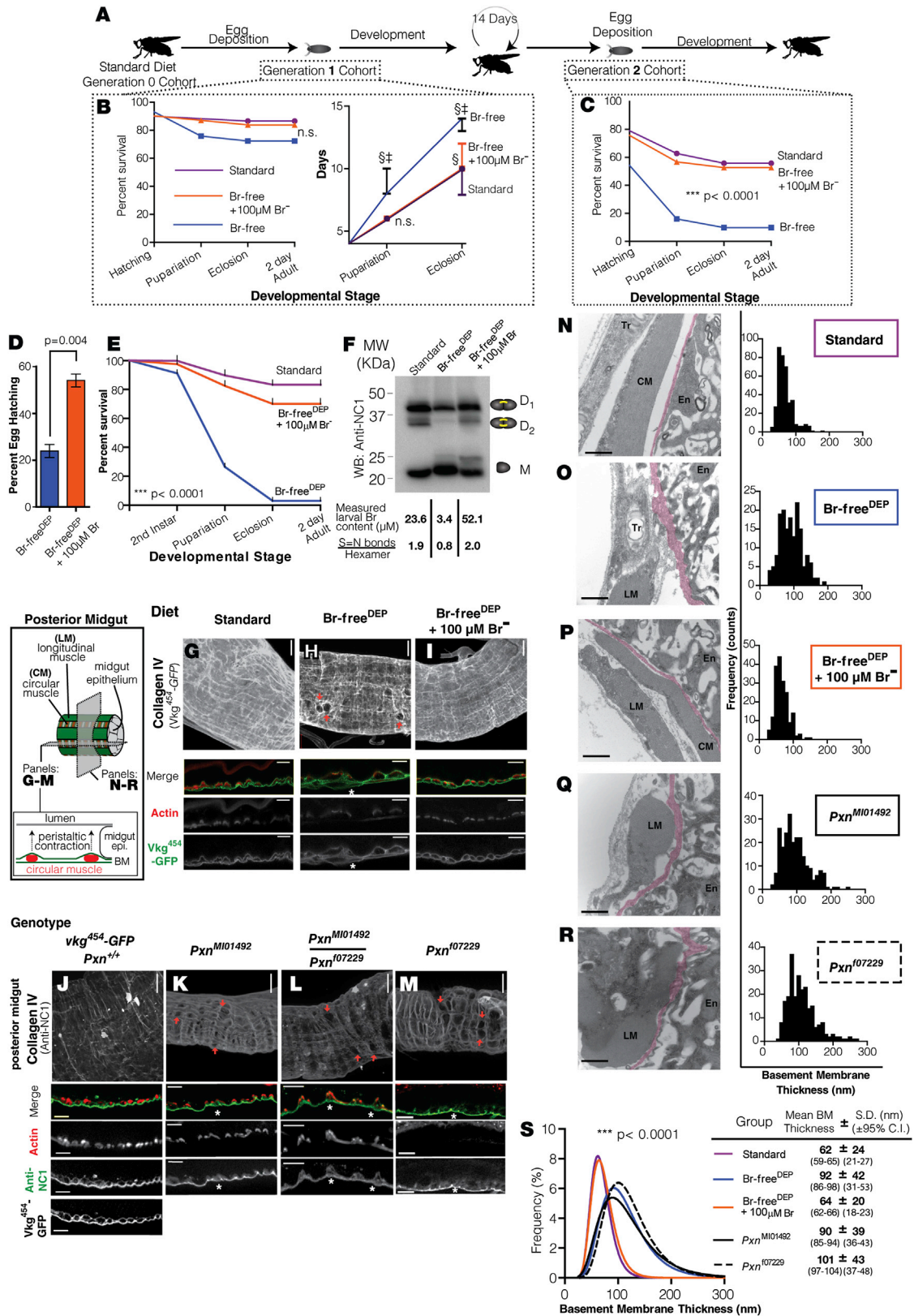
Seeking to accelerate Br⁻ depletion, we fed flies a Br-free diet containing elevated NaCl levels to reduce Br⁻ half-life in vivo via halide flux seen in mammals (Pavelka et al., 2005). Female *Drosophila* were placed on a Br⁻-depleting (Br-free^{DEP}) diet with or without supplemental 100 μ M Br⁻ prior to egg deposition, and the dietary conditions were maintained throughout progeny development. Initially, the Br-free^{DEP} egg cohort had a significantly reduced hatching percentage relative to Br-free^{DEP} + 100 μ M Br⁻ (Figure 5D), suggesting that Br⁻ is required for successful embryogenesis. Nearly all hatched larvae died prior

(C) Uncrosslinked NC1 hexamer (1.3 μ M) was reacted with indicated amounts of HOCl for 1 min at 37°C in Br-free 1 \times PBS, followed by subsequent treatment with 8 mol eq. HOBr (or HOCl as a control) and reacted for an additional minute at 37°C. Reactions were quenched with 20 mM methionine. Gel is representative of two experiments.

(D) The sequential model for D₁ and D₂ formation within the NC1 hexamer following complete stoichiometric oxidation of Met⁹³. P₁–P₄ indicate the proportional probabilities of forming the observed products. Calculations are presented in Extended Experimental Procedures.

(E) Free energy landscape for S = N formation within the NC1 hexamer based on the model outlined in (D) and Figures S5 and S6.

(F) Outline of overall chemical pathway governing the intrinsic chemical reactivity of **S-Br** and **S-Cl** at Met⁹³.



(legend on next page)

to eclosion under Br-free^{DEP} conditions, whereas 100 μ M Br⁻ rescued development to adulthood (Figure 5E). NAA analysis confirmed lower Br⁻ levels in third instar larvae (3.4 versus 23.6 μ M for controls) in Br-free^{DEP} conditions (Figure 5F).

In Br-free^{DEP} conditions, we assessed the impact of Br deficiency on crosslink formation in vivo. We used *vkg*⁴⁵⁴-GFP flies in which the single collagen IV α 2 gene locus contains a GFP insertion near the 7S domain. We grew these *vkg*⁴⁵⁴-GFP flies on Br-free^{DEP}, Br-free^{DEP} + 100 μ M Br⁻, and standard diets and biochemically assayed sulfilimine-bond content via immunoblot (Extended Experimental Procedures). We found grossly reduced sulfilimine-bond content in the Br-free^{DEP} cohort, which was rescued with Br⁻ supplementation (Figures 5F and S7A). Thus, Br⁻ promotes sulfilimine formation in vivo.

Peroxidasin (Pxn) mutants have reduced amounts of collagen IV sulfilimine crosslinks and consequent perturbation of midgut BM, as shown previously (*Pxn*^{f07229}, Bhave et al., 2012). Predicting that Br depletion would phenocopy the *Pxn* mutant, we compared the midgut from Br-free^{DEP} larvae to two independent mutants of *Pxn* (*Pxn*^{M101492} and *Pxn*^{f07229}). Although normal scaffold architecture was seen on standard diet (Figure 5G), Br-free^{DEP} conditions displayed gross disruptions (Figure 5H, red arrows) and splitting in the overall collagen IV scaffold (Figure 5H, asterisk). Both phenotypes were rescued in Br-free^{DEP} + 100 μ M Br⁻ media (Figure 5I). Significantly, similar disruptions were seen in *Pxn* mutants using an anti-NC1 antibody (Figures 5J–5M). The *Pxn*^{f07229} phenotype appeared more severe

than *Pxn*^{M101492}, and the *Pxn*^{M101492}/*Pxn*^{f07229} transheterozygote demonstrated an intermediate phenotype. These data indicate similarities between Br deficiency and the loss of peroxidase.

We used transmission electron microscopy (TEM) to compare the BM ultrastructure in Br-depleted larvae with *Pxn* mutant larvae. Larvae raised on standard diet exhibited normal enterocyte and BM structure (Shanbhag, and Tripathi, 2009) (Figure 5N). In Br-free^{DEP} larvae, the BM was irregular, thickened, occasionally diffuse, and wavy in various sections (Figure 5O). Strikingly, both *Pxn* mutants exhibited irregular and thickened BM similar to the Br-free^{DEP} cohort (Figures 5Q and 5R). Moreover, Br-free^{DEP} conditions and *Pxn* mutants displayed circular muscles protruding into and deforming the gut epithelium, (Figures 57C, 57E, and 57F), mirroring the actin staining in circular muscles (Figures 5H, 5K, and 5M). All sections from the Br-free^{DEP} + 100 μ M Br⁻ and standard-diet cohorts displayed normal BM and circular muscle morphologies (Figures 5N, 5P, 57B, and 57D). We quantified the BM morphologic changes observed by TEM, finding similar BM thickness in the standard and Br-free^{DEP} + 100 μ M Br⁻ diets but significantly thicker BMs in Br-free^{DEP} and both *Pxn* mutants (Figures 5S and 57G).

Br-free^{DEP} conditions phenocopy the genetic loss of *Pxn*, so we hypothesized that Br⁻ and *Pxn* interact in vivo to strengthen collagen IV scaffolds. It has been reported that collagen IV acts during *Drosophila* oogenesis as a “molecular corset” to control egg shape, restricting circumferential expansion so that egg growth promotes elongation along the anterior-posterior axis

Figure 5. Bromide Is Essential for Development and BM Architecture in *Drosophila*

(A) Generational Br-depletion scheme.

(B) Generation 1 survival and time-to-development curves for *w*¹¹¹⁸ flies on the standard diet versus experimental diets. Embryos from mothers fed a standard diet were placed on the indicated diet, and progeny were scored every 24 hr. There was not a significant difference in survival between groups by log-rank test (left panel). The Br-free + 100 μ M Br⁻ diet supported the same timing of development as the standard diet, whereas the Br-free diet caused a significant delay ($p < 0.001$ compared to both standard diet and Br-free + 100 μ M Br⁻) prior to pupariation (8 days) and eclosion (14 days) (right panel). Data plotted as the group median \pm interquartile range. $n = 30$ for each group. Two-way ANOVA test showed a significant difference for pupariation and eclosion ($p < 0.001$); $\ddagger =$ different from standard, $\ddagger\ddagger =$ different from Br-free + 100 μ M Br⁻.

(C) Generation 2 developmental survival on experimental diets. $n > 40$ for each cohort. Tested by log-rank test.

(D) Percentage of eggs (mean \pm 95% CI) completing embryogenesis from mothers reared on Br-free^{DEP} or Br-free^{DEP} + 100 μ M Br⁻ diets for 5 days. In the Br-free^{DEP} experimental group, mothers were fed Br-free synthetic diet containing 80 mM total NaCl (Br-free^{DEP}) for 3 days prior to egg collection. The Br-free^{DEP} + 100 μ M Br⁻ was treated in the same manner except that 100 μ M NaBr was added to all food components of the Br-free^{DEP} synthetic diet. Hatching rate differences were observed for eggs collected 3–7 days after maternal diet implementation. $n = 300$ eggs. Analyzed by the Mann-Whitney U test.

(E) Survival curve for *w*¹¹¹⁸ flies under standard, Br-free^{DEP}, and Br-free^{DEP} + 100 μ M Br⁻ dietary conditions. The survival difference between groups was highly significant (log-rank test, $n > 40$ for each group).

(F) Western blot of isolated NC1 domain from larvae treated as in (E), probed with an anti-*Drosophila* NC1 polyclonal antibody (Extended Experimental Procedures). Associated larval Br content was measured by EINAA (additional data in Table S2). Bonds/hexamer were calculated from the western blot.

(G–I) Representative images of *vkg*⁴⁵⁴-GFP homozygous larvae reared under the conditions tested in (E), demonstrating holes in the BM (indicated by orange arrows) in the distal posterior midgut of Br-free^{DEP} larvae. Optical sections of mid-lateral gut plane visualizing the circular muscles in cross-section (F-actin stained with phalloidin) surrounded by a collagen IV (*Vkg*⁴⁵⁴-GFP) scaffold and the gut epithelial BM. Gut lumen is oriented at the top of the image, anterior-posterior axis is horizontal. * = BM defect. Whole-gut images, scale bar represents 20 μ m; mid-lateral plane optical sections, scale bar represents 10 μ m.

(J–M) Representative images of posterior midgut of 4-day-old larvae with indicated peroxidase genotype on standard food. Collagen IV anti-NC1 staining on nonpermeabilized samples demonstrates BM staining similar to that of *Vkg*⁴⁵⁴-GFP (J). F-actin was stained with phalloidin. No muscle actin staining is visible in (M) due to muscle death, directly visualized by EM in (R). * = BM defect. Whole-gut images, scale bar represents 20 μ m; mid-lateral plane optical sections, scale bar represents 10 μ m.

(N–R) EMs of circular sections through the posterior midgut, focusing on the BM (magenta pseudocolor) beneath the enterocyte (En) near a longitudinal muscle belly (LM). Trachioles (Tr) are occasionally visualized. Standard diet control (N) has a compact, normal BM. BMs are thickened and irregular in Br-free^{DEP} (O), *Pxn*^{M101492} (Q), and *Pxn*^{f07229} (R); BM is similar to control in Br-free^{DEP} + 100 μ M Br⁻ (P). BMs from 15 independent sections for each group were evaluated for thickness, and the histograms plotted. Scale bar represents 0.5 μ m.

(S) Distribution curves and parameters from fitted distributions of each experimental group. Optimal Box-Cox transformations were performed for normality, and the transformed distributions were fitted. The curves to fit the data were significantly different by the F test. Pairwise comparison revealed no significant difference between standard and Br-free^{DEP} + 100 μ M Br⁻, whereas both curves differed significantly from Br-free^{DEP}, *Pxn*^{M101492}, and *Pxn*^{f07229}. Bootstrapping was performed to obtain the 95% CIs for the mean and SD for each group, revealing that the variance in BM thickness in Br-free^{DEP}, *Pxn*^{M101492}, and *Pxn*^{f07229} is substantially higher. (See also Figure S7.)

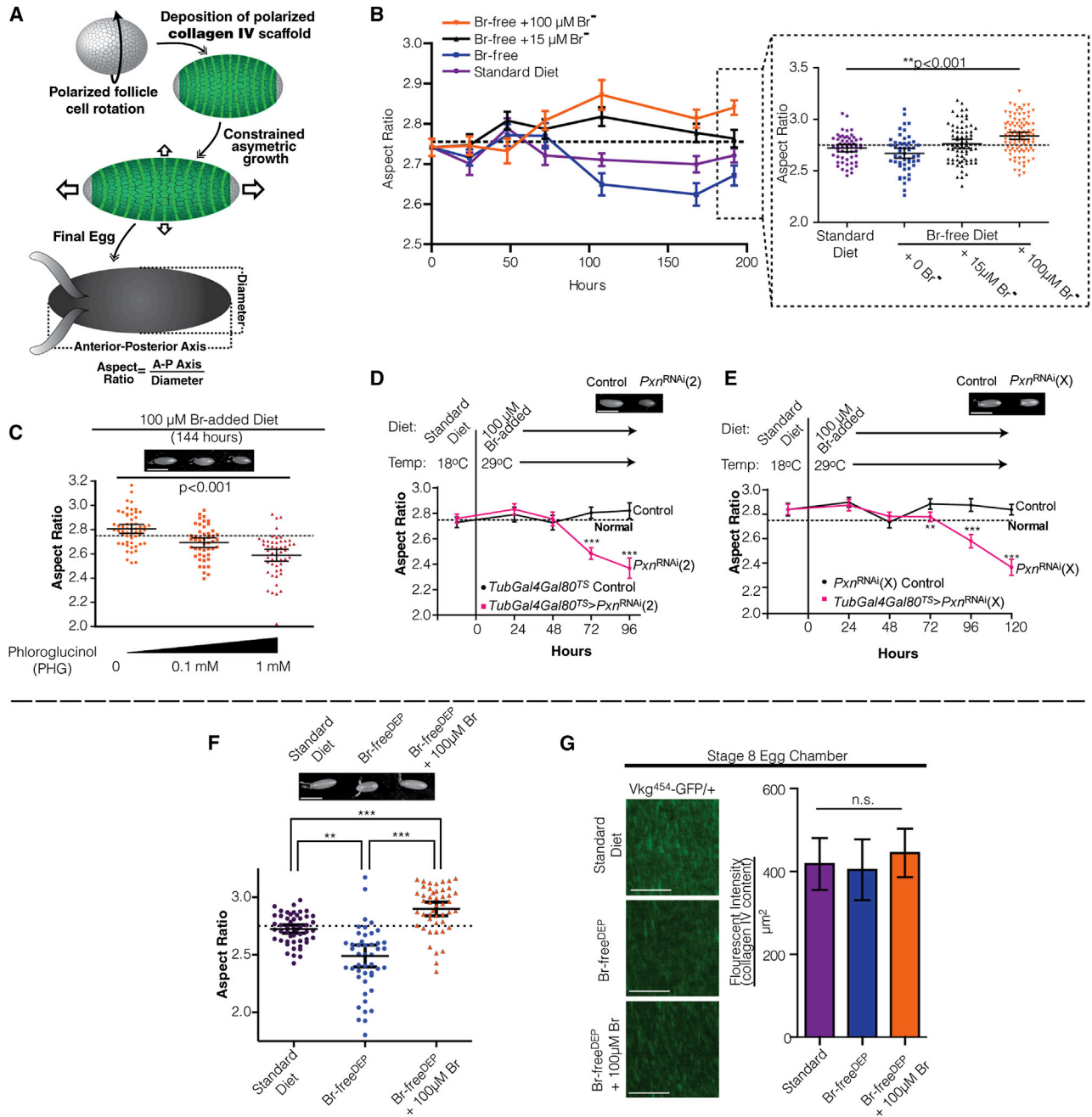


Figure 6. Br^- and Peroxidase Interact In Vivo to Strengthen Collagen IV Scaffolds

(A) Schematic overview of polarized collagen IV scaffolds (molecular corset, green), which determine aspect ratio in *Drosophila* eggs. (B) Br^- concentration effect on egg aspect ratio, in single age-matched cohort of w^{1118} flies, over time. Vertical axis represents mean aspect ratio (\pm SEM). At 192 hr (inset), egg aspect ratio had increased proportionally to Br^- concentration, with similar aspect ratios in 15 μM -added NaBr and standard diet (measured as 15 μM Br^- by NAA). Inset plotted as mean \pm 95% CI, and significance calculated with the Kruskal-Wallis test. Dotted line indicates egg aspect ratio reported by Haigo and Bilder (2011).

(C) An irreversible peroxidase inhibitor, PHG, causes a dose-dependent reduction in the exaggerated egg elongation caused by excess dietary (100 μM) Br^- . PHG was administered in the food. All wild-type (w^{1118}) mothers were from the same cohort and reared identically, then divided into sub-cohorts for exposure to the indicated experimental diet. Significance among the conditions was calculated using the Kruskal-Wallis test. Data plotted as mean \pm 95% CI (image; scale bar represents 500 μm). Dotted line indicates reported value for egg aspect ratio (Haigo and Bilder, 2011). All groups also differed significantly when compared individually using Dunn's multiple comparison testing ($p < 0.05$).

(D and E) Pxn is required for Br-induced egg elongation. Two independent temperature-inducible RNAi constructs targeting *Pxn* were expressed in adult females fed 100 μM added Br^- . Aspect ratios from maternally expressed *Pxn*^{RNAi} were significantly different than sibling-matched controls after induction for 72 hr (29°C)

(legend continued on next page)

(Figure 6A) (Haigo and Bilder, 2011). In eggs from mothers fed varying concentrations of Br^- , we found a dose-dependent relationship between Br^- and aspect ratio (Figure 6B) after approximately 4 days, consistent with a long biologic half-life for Br^- . Interestingly, the aspect ratio of eggs on the Br-added diet (100 μM Br^-) exceeded the ratio for eggs on standard diet (NAA measured 15 μM Br^- ; Table S2) (Figure 6B), suggesting that elevated Br^- promotes additional sulfilimine formation to enhance tensile strength in the collagen IV molecular corset.

We used this elongated egg aspect ratio to probe whether Br^- and Pxn act via a common mechanism in strengthening collagen IV. We used two methods to assess whether Pxn is required for the elongation phenotype. First, we used an irreversible inhibitor, phloroglucinol, to inhibit peroxidase activity, and we observed a dose-dependent suppression in egg aspect ratio in the presence of elevated Br^- (Figure 6C). Second, to confirm the specificity of this interaction, we used two separate ubiquitously driven temperature-sensitive conditional RNAi constructs to knock down peroxidase in adult females in the presence of 100 μM Br^- . In both RNAi experiments, aspect ratio was significantly decreased relative to controls 3–4 days after the onset of *Pxn* knockdown (Figures 6D, 6E, and S7), whereas controls displayed normal augmentation of aspect ratio under identical conditions. Thus Pxn is required for the Br-induced elongation phenotype. To address the alternative hypothesis that Br^- levels modulate collagen IV deposition, we examined Vkg-GFP immunofluorescence in eggs from mothers raised on Br-free^{DEP} media. Like the Br-deficient diet, the Br-free^{DEP} media reduced egg aspect ratio (Figure 6F), but collagen IV content appeared similar to controls (Figure 6G) after 1 week of maternal exposure to Br-free^{DEP} diet, suggesting that the egg aspect-ratio phenotypes are caused by structural deficiencies within the scaffold.

DISCUSSION

Essentiality and Function of Bromide in Animals

We provide evidence that bromine is essential in animals, satisfying the principal requirements for elemental essentiality: (1) demonstration that elemental deficiency leads to physiologic dysfunction, (2) repletion of the element that reverses dysfunction, and (3) biochemical explanation of the physiologic function (Mertz, 1981). Br-deficient *Drosophila* display altered BM and tissue morphology, aberrant embryogenesis, larval mid-gut defects, and lethality, whereas Br^- repletion restored normal development. Mechanistically, the assembly of crosslinked collagen IV scaffolds requires Br^- .

Sulfilimine-crosslinked collagen IV scaffolds are central to the form and function of BMs in animals (Bhave et al., 2012; Fidler

et al., 2014). Our data indicate that the crosslink stabilizes nascent collagen IV scaffolds, effectively modulating scaffold assembly and BM thickness. Because sulfilimine formation involves the concerted activity of collagen IV, Br^- , peroxidase, and oxidant, we view each as critical for BM assembly and tissue development (Figures 7A and 7B).

Mechanistic Role of Bromide in Sulfilimine Formation

The requirement for Br^- during sulfilimine formation derives from the selectivity of the bromosulfonium reaction intermediate. The chemical character of bromine uniquely creates an energetically favorable reaction between the **S-Br** intermediate and Hyl^{211} . The **S-Br** molecular orbital structure facilitates selective reactivity with an amine nucleophile to form the crosslink, contrasting with the highly polar **S-Cl** intermediate that preferentially forms a sulfoxide via charge-controlled reaction with water (Figure 7C). Peroxidase harnesses this HOBr-based selectivity during crosslinking while apparently avoiding oxidative damage to the BM.

Bromide Homeostasis

Br^- is mainly located extracellularly and has been used in the clinical measurement of extracellular volume (Barratt and Walser, 1969; Brodie et al., 1939). Plasma Br^- is 67 μM in healthy people, congruent with Br^- concentrations that support sulfilimine formation in flies, and are maintained within an order of magnitude in many species (freshwater fish [Woods et al., 1979], flies [Piedade-Guerreiro et al., 1987], rodents [van Logten et al., 1974], and humans [Olszowy et al., 1998; van Leeuwen and Sangster, 1987]). In humans, plasma Br^- is maintained via diet and renal excretion (Trautner and Wieth, 1968; van Leeuwen and Sangster, 1987; Walser and Rahill, 1966; Wolf and Eadie, 1950). *Drosophila* likely conserve Br^- , possibly contributing to the timeline of phenotype development in our generational dietary Br-deficiency model (Figures 5A–5C). Dietary Br deficiency has been suggested to suppress tissue growth and increase lethality in goats (Anke et al., 1990), whereas high-serum Br^- (>12 mM) causes neurologic and dermatologic complications (van Leeuwen and Sangster, 1987). Taken together, this implies that an optimal Br^- concentration might exist and is regulated in vivo.

Clinical Implications of Bromide Deficiency

Bromide deficiency may have implications in human health and disease. Patients receiving total parenteral nutrition (TPN) are reported to have low plasma Br^- levels due to lower dietary Br consumption (Dahlstrom et al., 1986), and end-stage renal disease patients have enhanced Br^- losses as a consequence of dialysis (Miura et al., 2002; Oe et al., 1981; Wallaeyts et al.,

by Mann-Whitney U test. * $p < 0.05$, *** $p < 0.001$. Data plotted as mean \pm 95% CI (inset image scale bar represents 500 μm). Dotted line indicates reported value for egg aspect ratio (Haigo and Bilder, 2011).

(F) Egg aspect ratio on standard diet and synthetic Br-free^{DEP} and Br-free^{DEP} + 100 μM Br^- diets. Eggs were collected after mothers were fed indicated diet for 7 days. Differences in egg aspect ratio were observed in eggs collected after 5–7 days of experimental diets. Representative pictures of eggs are shown (scale bar represents 500 μm). Aspect ratio plotted as mean \pm 95% CI (graph; Mann Whitney U test; ** $p < 0.01$ *** $p < 0.001$). Dotted line indicates reported value for egg aspect ratio (Haigo and Bilder, 2011).

(G) Collagen IV density appears normal in eggs from Br-depleted mothers. BM of stage 8 egg chambers from mothers expressing Vkg-GFP and fed the indicated diet are shown (confocal images). For quantitation, fluorescence intensities of z stack projections were summed in areas where the whole thickness of the BM had been observed and normalized to the observational area. $n = 9$ for each group. There was no difference in the medians between the groups by the Kruskal-Wallis test. Data plotted as mean \pm 95% CI (image; scale bar represents 20 μm). See also Figure S7.

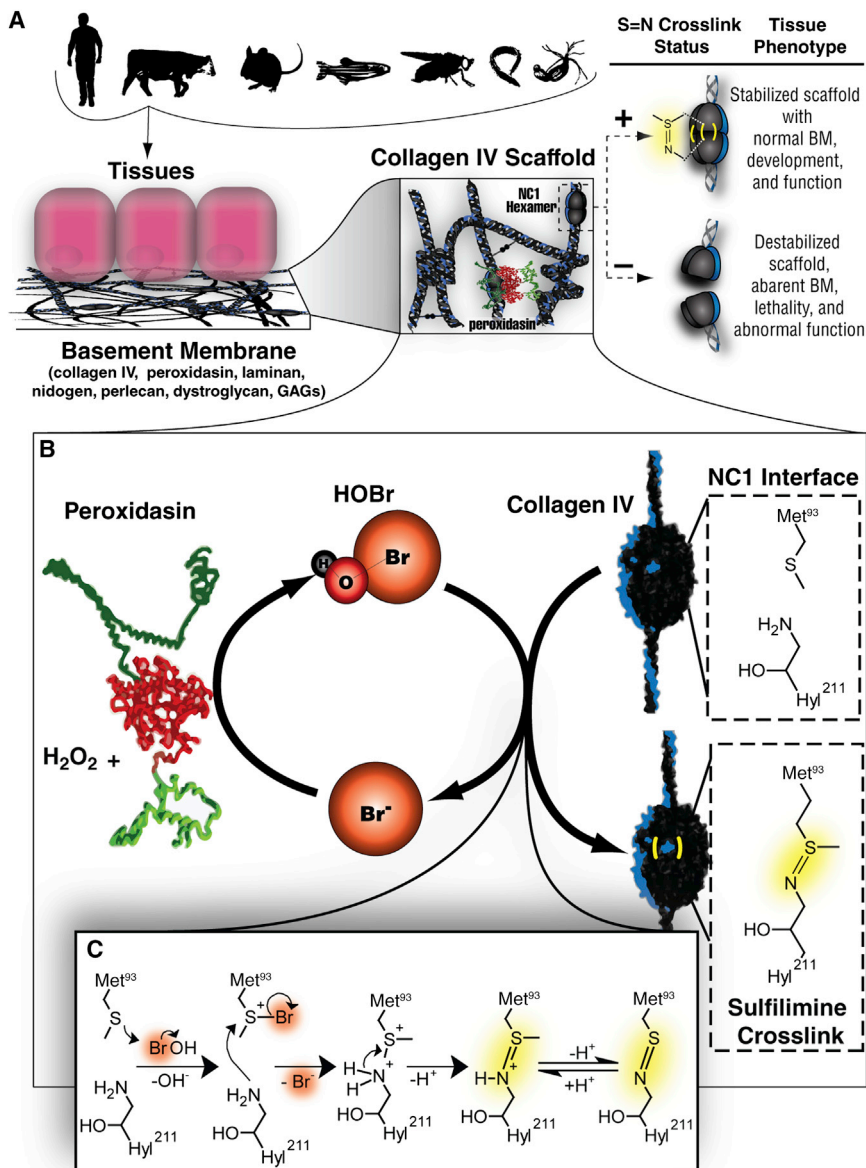


Figure 7. Model of the Essentiality of Bromine in Forming Collagen IV Sulfilimine Crosslinks

(A) Diagrammatic relationship between collagen IV sulfilimine formation and tissue phenotype. (B) Schematic representation of role of bromide in oxidative formation of sulfilimine crosslinks. (C) Proposed chemical mechanism of sulfilimine formation by HOBr.

sen, 1979; Soltani et al., 2012). Finally, because BM assembly involves Br^- , tissue development or remodeling may be vulnerable to Br deficiency. The findings of our study provide rationale for investigating the clinical implications of Br deficiency and the physiologic consequences of mechanically perturbing collagen IV scaffolds.

EXPERIMENTAL PROCEDURES

Detailed Experimental Procedures for materials and methods appear in the [Extended Experimental Procedures](#) online.

High-Resolution Mass Spectrometry

NC1 domains were resolved by SDS-PAGE, excised, and “in-gel” trypsin digested as described (Vanacore et al., 2009). The resultant sample was enriched for sulfilimine-crosslinked peptides and analyzed using LC-MS. Data analysis using a combination of Thermo Xcalibur 2.1, the Myrimatch algorithm with Bumpershoot suite, Scaffold, (Proteome Software, Portland, OR, USA), ScanRanker, and IonMatcher software, where appropriate.

Br-free Salt Purification

Concentrated solutions of metal (Na, K) hydroxide and reagent-grade HCl were placed in a sealed chamber that prevented liquid mixing yet allowed vapor diffusion (Figures 2C and S3). After 4 days, sufficient HCl vapor had diffused and reacted

1986). Because Br has not been considered an essential trace element, systematic investigations on Br^- replacement have not been pursued in these disease states (Nielsen, 1998). Intriguingly, TPN alters intestinal mucosal architecture and function in a manner reminiscent of the mid-gut phenotypes of *Drosophila Pxn* mutants and Br-deficient larvae (Groos et al., 2003). Furthermore, functional Br^- deficiency may occur in smokers in spite of normal plasma Br^- levels because of elevated levels of serum SCN^- , which inhibits sulfilimine bond formation. In our present study, we found SCN^- to be a potent inhibitor of peroxidasin-mediated crosslink formation (Figures 2A and S2). Therefore, in some smokers with elevated SCN^- levels (130 μM , 1 pack per day) (Tsuge et al., 2000), reinforcement of collagen IV scaffolds with sulfilimine crosslinks may be substantially reduced (see [Extended Experimental Procedures](#)). Indeed, smoking has been associated with architectural changes within BMs (Asmus-

to neutralize the OH^- , and the resultant metal Cl^- salt was assayed for purity via ICP-MS (Table S1).

PFHR-9 Cell Culture/Collagen Matrix Preparation

PFHR-9 cells (ATCC CRL-2423) were cultured in Dulbecco’s modified Eagle’s medium (DMEM) with 5% FBS under 10% CO_2 . Collagen IV was deposited in culture for 7–9 days with daily media changes. Uncrosslinked hexamer was generated by culturing cells in either 50 μM phloroglucinol (PHG) or 1 mM KI. Br-free DMEM for cell culture was prepared as per [Tables S3 and S4](#).

Protein Purification

Recombinant human peroxidasin (hPXDN) was expressed in HEK293 cells and purified as described previously (Bhave et al., 2012), with Br-free buffers used as appropriate in chromatography, dialysis, and centrifugation steps. Purified enzyme was reacted in vitro with uncrosslinked NC1 generated in PHG-treated PFHR-9 culture. Uncrosslinked hexamers were isolated with collagenase digestion and purified by subsequent chromatography in normal or Br-free buffers ([Extended Experimental Procedures](#)).

Chemical Crosslinking of NC1 Domains by Hypohalous Acids

Uncrosslinked NC1 was reacted with hypohalous acid for 1 min at 37°C, quenched with methionine, and analyzed by SDS-PAGE. HOBr was prepared as previously described (Bhave et al., 2012). Detailed methods for densitometric analysis and thermodynamic calculations are in the [Extended Experimental Procedures](#).

Br-free *Drosophila* Food

S. cerevisiae was cultured in adapted Br-free yeast nitrogen base (YNB) media (Table S6). Phytigel-based fly media contained additional vitamins and minerals (Table S7) plus ampicillin and Tegocept. Br-free NaCl and KCl were the only sources of chloride in the fly media. The combination of Br-free yeast and phytigel was used for both larval and adult rearing. Final media Br⁻ levels were undetectable by NAA (Table S2).

Drosophila Genetics and Methods

see [Extended Experimental Procedures](#) for details.

Statistical Analysis

Analysis performed in this work was completed in GraphPad Prism v. 5.00 for Windows (GraphPad Software, San Diego, CA, USA) and SPSS v. 22 (IBM). All statistical tests between groups were analyzed using nonparametric measures indicated unless the data were found to be normal.

SUPPLEMENTAL INFORMATION

Supplemental Information includes Extended Experimental Procedures, seven figures, seven tables, and supplemental references and can be found with this article online at <http://dx.doi.org/10.1016/j.cell.2014.05.009>.

AUTHOR CONTRIBUTIONS

All authors contributed as a team to experimental design, interpretation of data, and writing of manuscript. A.S.M. lead the effort on Br essentiality and chemical mechanisms. C.F.C. lead the effort on the initial observations of Br function in collagen IV crosslinking. G.B. designed the Br-free Cl purification method, all Br-free methods and their application to the overall project. A.S.M. and R.V. conducted mass spectrometry experiments. A.S.M., G.B., and A.P.-M. designed and conducted *Drosophila* experiments.

ACKNOWLEDGMENTS

This work was supported by the following: NIH R01 DK18381 to B.G.H.; NIH F30 DK100094-01 to A.S.M.; NIGMS T32 GM07347 to the Vanderbilt Medical-Scientist Training Program and the Canby Robinson Society in support of A.S.M.; NIH KO8 DK097306 and the Vanderbilt Physician Scientist Development Award to G.B.; and NIH R01 GM073883 to A.P.-M. We are grateful to K.L. Rose at Vanderbilt Mass Spectrometry Resource Center; J. Clanton, X. Wang, and E. Shannon for assistance with *Drosophila*; J. Williams and W.G. Jerome for assistance with Electron Microscopy and sample preparation, performed with use of the VUMC Cell Imaging Shared Resource; and the Bloomington *Drosophila* Stock Center, Yale Fly Trap, and the VDRC for fly stocks. The technical assistance of P. Todd and M. Rafi is appreciated. We acknowledge S. Kraft for helpful chemistry discussions. C.F.C. and B.G.H. are cofounders of SULFILATEC, INC. C.F.C. is a director and officer without salary of SULFILATEC, INC.

Received: October 15, 2013

Revised: February 14, 2014

Accepted: March 25, 2014

Published: June 5, 2014

REFERENCES

Anke, M., Regius, Á., Groppe, B., and Arnhold, W. (1990). Essentiality of the trace element bromine. *Acta Agronomica Hung.* 39, 297–303.

Armesto, X.L., Canle, L.M., Fernandez, M.I., Garca, M.V., and Santaballa, J.A. (2000). First steps in the oxidation of sulfur-containing amino acids by hypohalogenation: very fast generation of intermediate sulfonyl halides and halosulfonium cations. *Tetrahedron* 56, 1103–1109.

Asmussen, I. (1979). Fetal cardiovascular system as influenced by maternal smoking. *Clin. Cardiol.* 2, 246–256.

Barratt, T.M., and Walsler, M. (1969). Extracellular fluid in individual tissues and in whole animals: the distribution of radiolabeled sulfate and radiobromide. *J. Clin. Invest.* 48, 56–66.

Bhave, G., Cummings, C.F., Vanacore, R.M., Kumagai-Cresse, C., Ero-Tolliver, I.A., Rafi, M., Kang, J.S., Pedchenko, V., Fessler, L.I., Fessler, J.H., and Hudson, B.G. (2012). Peroxidase forms sulfonamide chemical bonds using hypohalous acids in tissue genesis. *Nat. Chem. Biol.* 8, 784–790.

Borchiellini, C., Coulon, J., and Le Parco, Y. (1996). The function of type IV collagen during *Drosophila* muscle development. *Mech. Dev.* 58, 179–191.

Bozeman, P.M., Learn, D.B., and Thomas, E.L. (1990). Assay of the human leukocyte enzymes myeloperoxidase and eosinophil peroxidase. *J. Immunol. Methods* 126, 125–133.

Brodie, B.B., Brand, E., and Leshin, S. (1939). The use of bromide as a measure of extracellular fluid. *J. Biol. Chem.* 130, 555–563.

Chmutova, G., Ziganshina, A.Y., and Movchan, A. (1999). Differences in the electronic structure of sulfonyl chlorides and bromides as possible reasons for their different reactivities toward aromatic compounds. *Russ. J. Org. Chem.* 35, 56–61.

Dahlstrom, K.A., Ament, M.E., Medhin, M.G., and Meurling, S. (1986). Serum trace elements in children receiving long-term parenteral nutrition. *J. Pediatr.* 109, 625–630.

Daley, W.P., and Yamada, K.M. (2013). ECM-modulated cellular dynamics as a driving force for tissue morphogenesis. *Curr. Opin. Genet. Dev.* 23, 408–414.

Fidler, A.L., Vanacore, R.M., Chetyrkin, S.V., Pedchenko, V.K., Bhave, G., Yin, V.P., Stothers, C.L., Rose, K.L., McDonald, W.H., Clark, T.A., et al.; Aspirin (2014). A unique covalent bond in basement membrane is a primordial innovation for tissue evolution. *Proc. Natl. Acad. Sci. USA* 111, 331–336.

Gotenstein, J.R., Swale, R.E., Fukuda, T., Wu, Z., Giurumescu, C.A., Goncharov, A., Jin, Y., and Chisholm, A.D. (2010). The *C. elegans* peroxidase PNX-2 is essential for embryonic morphogenesis and inhibits adult axon regeneration. *Development* 137, 3603–3613.

Gould, D.B., Phalan, F.C., Breedveld, G.J., van Mil, S.E., Smith, R.S., Schimenti, J.C., Aguglia, U., van der Knaap, M.S., Heutink, P., and John, S.W. (2005). Mutations in Col4a1 cause perinatal cerebral hemorrhage and porencephaly. *Science* 308, 1167–1171.

Groos, S., Reale, E., Hünefeld, G., and Luciano, L. (2003). Changes in epithelial cell turnover and extracellular matrix in human small intestine after TPN. *J. Surg. Res.* 109, 74–85.

Gupta, M.C., Graham, P.L., and Kramer, J.M. (1997). Characterization of alpha1(IV) collagen mutations in *Caenorhabditis elegans* and the effects of alpha1 and alpha2(IV) mutations on type IV collagen distribution. *J. Cell Biol.* 137, 1185–1196.

Haigo, S.L., and Bilder, D. (2011). Global tissue revolutions in a morphogenetic movement controlling elongation. *Science* 331, 1071–1074.

Hudson, B.G., Tryggvason, K., Sundaramoorthy, M., and Neilson, E.G. (2003). Alport's syndrome, Goodpasture's syndrome, and type IV collagen. *N. Engl. J. Med.* 348, 2543–2556.

Hynes, R.O. (2009). The extracellular matrix: not just pretty fibrils. *Science* 326, 1216–1219.

Klopman, G. (1968). Chemical reactivity and the concept of charge- and frontier-controlled reactions. *J. Am. Chem. Soc.* 90, 223–234.

Langeveld, J.P., Wieslander, J., Timoneda, J., McKinney, P., Butkowski, R.J., Wisdom, B.J., Jr., and Hudson, B.G. (1988). Structural heterogeneity of the noncollagenous domain of basement membrane collagen. *J. Biol. Chem.* 263, 10481–10488.

- Lin, C.Q., and Bissell, M.J. (1993). Multi-faceted regulation of cell differentiation by extracellular matrix. *FASEB J.* *7*, 737–743.
- Mayeno, A.N., Curran, A.J., Roberts, R.L., and Foote, C.S. (1989). Eosinophils preferentially use bromide to generate halogenating agents. *J. Biol. Chem.* *264*, 5660–5668.
- Mertz, W. (1981). The essential trace elements. *Science* *213*, 1332–1338.
- Miura, Y., Nakai, K., Suwabe, A., and Sera, K. (2002). Trace elements in renal disease and hemodialysis. *Nucl. Instrum. Meth. B* *189*, 443–449.
- Nagy, P., Beal, J.L., and Ashby, M.T. (2006). Thiocyanate is an efficient endogenous scavenger of the phagocytic killing agent hypobromous acid. *Chem. Res. Toxicol.* *19*, 587–593.
- Nielsen, F.H. (1998). Ultratrace elements in nutrition: Current knowledge and speculation. *J. Trace Elem. Exp. Med.* *11*, 251–274.
- Oe, P., Vis, R., Meijer, J., Van Langevelde, F., Allon, W., and Meer Cvd, V.H. (1981). Bromine deficiency and insomnia in patients on dialysis. In *Trace Element Metabolism in Man and Animals* (Canberra, Australia: TEMA-4 Australian Academy of Science), pp. 526–529.
- Olszowy, H.A., Rossiter, J., Hegarty, J., and Geoghegan, P. (1998). Background levels of bromide in human blood. *J. Anal. Toxicol.* *22*, 225–230.
- Pastor-Pareja, J.C., and Xu, T. (2011). Shaping cells and organs in *Drosophila* by opposing roles of fat body-secreted collagen IV and perlecan. *Dev. Cell* *21*, 245–256.
- Pearson, R.G. (1968). Hard and soft acids and bases, HSAB, part I: fundamental principles. *J. Chem. Educ.* *45*, 581.
- Peskin, A.V., Turner, R., Maghzal, G.J., Winterbourn, C.C., and Kettle, A.J. (2009). Oxidation of methionine to dehydromethionine by reactive halogen species generated by neutrophils. *Biochemistry* *48*, 10175–10182.
- Pavelka, S., Babický, A., and Vobecký, M. (2005). Biological half-life of bromide in the rat depends primarily on the magnitude of sodium intake. *Physiol. Res.* *54*, 639–644.
- Piedade-Guerreiro, J., Carmo Freitas, M., and Martinho, E. (1987). Application of NAA in determining the inorganic contents of the fruit fly (*Ceratitidis capitata* Wied.) and its artificial food. *J. Radioanal. Nucl. Chem.* *110*, 531–537.
- Pöschl, E., Schlötzer-Schrehardt, U., Brachvogel, B., Saito, K., Ninomiya, Y., and Mayer, U. (2004). Collagen IV is essential for basement membrane stability but dispensable for initiation of its assembly during early development. *Development* *131*, 1619–1628.
- Rodriguez, A., Zhou, Z., Tang, M.L., Meller, S., Chen, J., Bellen, H., and Kimbrell, D.A. (1996). Identification of immune system and response genes, and novel mutations causing melanotic tumor formation in *Drosophila melanogaster*. *Genetics* *143*, 929–940.
- Seeman, J.I. (1983). Effect of conformational change on reactivity in organic chemistry. Evaluations, applications, and extensions of Curtin-Hammett Winstein-Holness kinetics. *Chem. Rev.* *83*, 83–134.
- Shanbhag, S., and Tripathi, S. (2009). Epithelial ultrastructure and cellular mechanisms of acid and base transport in the *Drosophila* midgut. *J. Exp. Biol.* *212*, 1731–1744.
- Soltani, A., Muller, H.K., Sohal, S.S., Reid, D.W., Weston, S., Wood-Baker, R., and Walters, E.H. (2012). Distinctive characteristics of bronchial reticular basement membrane and vessel remodelling in chronic obstructive pulmonary disease (COPD) and in asthma: they are not the same disease. *Histopathology* *60*, 964–970.
- Song, J.J., and Ott, H.C. (2011). Organ engineering based on decellularized matrix scaffolds. *Trends Mol. Med.* *17*, 424–432.
- Trautner, M., and Wieth, J.O. (1968). Renal excretion of chloride, bromide and thiocyanate during water diuresis. *Acta Physiol. Scand.* *74*, 606–615.
- Tsuge, K., Kataoka, M., and Seto, Y. (2000). Cyanide and thiocyanate levels in blood and saliva of healthy adult volunteers. *J. Health Sci.* *46*, 343–350.
- van Leeuwen, F.X., and Sangster, B. (1987). The toxicology of bromide ion. *Crit. Rev. Toxicol.* *18*, 189–213.
- van Logten, M.J., Wolthuis, M., Rauws, A.G., Kroes, R., den Tonkelaar, E.M., Berkvens, H., and van Esch, G.J. (1974). Semichronic toxicity study of sodium bromide in rats. *Toxicology* *2*, 257–267.
- Vanacore, R., Ham, A.J., Voehler, M., Sanders, C.R., Conrads, T.P., Veenstra, T.D., Sharpless, K.B., Dawson, P.E., and Hudson, B.G. (2009). A sulfilimine bond identified in collagen IV. *Science* *325*, 1230–1234.
- Vracko, R. (1974). Basal lamina scaffold-anatomy and significance for maintenance of orderly tissue structure. *Am. J. Pathol.* *77*, 314–346.
- Wallaey, B., Cornelis, R., Mees, L., and Lameire, N. (1986). Trace elements in serum, packed cells, and dialysate of CAPD patients. *Kidney Int.* *30*, 599–604.
- Walsler, M., and Rahill, W.J. (1966). Renal tubular reabsorption of bromide compared with chloride. *Clin. Sci.* *30*, 191–205.
- Wang, X., Harris, R.E., Bayston, L.J., and Ashe, H.L. (2008). Type IV collagens regulate BMP signalling in *Drosophila*. *Nature* *455*, 72–77.
- Weiss, S.J., Test, S.T., Eckmann, C.M., Roos, D., and Regiani, S. (1986). Brominating oxidants generated by human eosinophils. *Science* *234*, 200–203.
- Werb, Z. (1997). ECM and cell surface proteolysis: regulating cellular ecology. *Cell* *91*, 439–442.
- Wolf, R.L., and Eadie, G.S. (1950). Reabsorption of bromide by the kidney. *Am. J. Physiol.* *163*, 436–441.
- Woods, A.E., Carlton, R.F., Casto, M.E., and Gleason, G.I. (1979). Environmental bromine in freshwater and freshwater organisms: factors affecting bioaccumulation. *Bull. Environ. Contam. Toxicol.* *23*, 179–185.
- Young, P.R., and Hsieh, L.-S. (1978). General base catalysis and evidence for a sulfurane intermediate in the iodine oxidation of methionine. *J. Am. Chem. Soc.* *100*, 7121–7122.
- Yurchenco, P.D. (2011). Basement membranes: cell scaffoldings and signaling platforms. *Cold Spring Harb. Perspect. Biol.* *3*, 3.